JCB **Article**

Proteolytic exposure of a cryptic site within collagen type IV is required for angiogenesis and tumor growth in vivo

Jingsong Xu,[1] Dorothy Rodriguez,[1] Eric Petitclerc,[1] Jenny J. Kim,[1] Masanori Hangai,[2] S. Moon Yuen,[2] George E. Davis,[3] and Peter C. Brooks[1]

[1]Departments of Radiation Oncology and Cell Biology, Kaplan Cancer Center, New York University School of Medicine, New York, NY 10016
[2]Department of Ophthamology, Doheny Eye Institute, University of Southern California, Los Angeles, CA 90033
[3]Department of Pathology and Laboratory Medicine, Texas A & M University Health Science Center, College Station, TX 77843

Evidence is provided that proteolytic cleavage of collagen type IV results in the exposure of a functionally important cryptic site hidden within its triple helical structure. Exposure of this cryptic site was associated with angiogenic, but not quiescent, blood vessels and was required for angiogenesis in vivo. Exposure of the HUIV26 epitope was associated with a loss of $\alpha 1\beta 1$ integrin binding and the gain of $\alpha v\beta 3$ binding. A monoclonal antibody (HUIV26) directed to this site disrupts integrin-dependent endothelial cell interactions and potently inhibits angiogenesis and tumor growth. Together, these studies suggest a novel mechanism by which proteolysis contributes to angiogenesis by exposing hidden regulatory elements within matrix-immobilized collagen type IV.

Introduction

The extracellular matrix (ECM)* is an interconnected molecular network that not only provides mechanical support for cells and tissues, but also regulates biochemical and cellular processes such as adhesion, migration, gene expression, and differentiation (Timpl and Brown, 1995; Timpl, 1996; Herbst et al., 1998; Tsai, 1998; Dogic et al., 1999). A specialized form of the ECM that separates epithelia from its underlying mesenchyme and lines blood vessels is the basement membrane (Timpl and Brown, 1995; Timpl, 1996). Although considerable progress has been made in understanding the roles of growth factors and integrin receptors in the process of angiogenesis, little is known concerning the role that basement membrane degradation plays in this process. Matrix degradation may simply provide a mechanism to remove a restrictive physical barrier that limits endothelial motility. Alternatively, ECM remodeling may release matrix-sequestered growth factors that promote endothelial cell proliferation and migration. However, the possibility that matrix remodeling does not simply destroy matrix barrier, but rather selectively exposes cryptic protein sequences that play an functional role in angiogenesis has not been explored in depth.

A major component of the vascular basement membrane is collagen type IV (Hudson et al., 1993). The most widely expressed form is composed of two $\alpha 1$(IV) chains and one $\alpha 2$(IV) chain and is found in the basement membrane of virtually all blood vessels. Interestingly, the triple helical nature of collagen is thought to regulate integrin-mediated cellular interactions (Messent et al., 1998; Emsley et al., 2000). In fact, proteolytic cleavage and denaturation can convert triple helical collagen type I from a $\beta 1$ integrin–directed ECM ligand to an $\alpha v\beta 3$-dependent ligand (Davis, 1992; Montgomery et al., 1994). This shift in integrin-mediated interactions may represent an important regulatory mechanism to activate distinct signal transduction pathways necessary for invasive cellular behavior. However, no direct evidence is available to indicate that interaction of denatured collagen with endothelial cells is a functionally important step in angiogenesis.

Here, we provide evidence that proteolytic cleavage of collagen type IV can expose a cryptic site which is normally hidden within its triple helical structure. This cryptic site was

Address correspondence to Peter C. Brooks, Departments of Radiation Oncology and Cell Biology, Kaplan Cancer Center, Rusk Building Room 806, New York University School of Medicine, 400 East 34th St., New York, NY 10016. Tel.: (212) 263-3021. Fax: (212) 263-3018. E-mail: peter.brooks@med.nyu.edu

*Abbreviations used in this paper: CAM, chorioallantoic membrane; ECM, extracellular matrix; HUVEC, human umbilical vein endothelial cell; MMP, matrix metalloproteinase; SCID, severe combined immunodeficient.

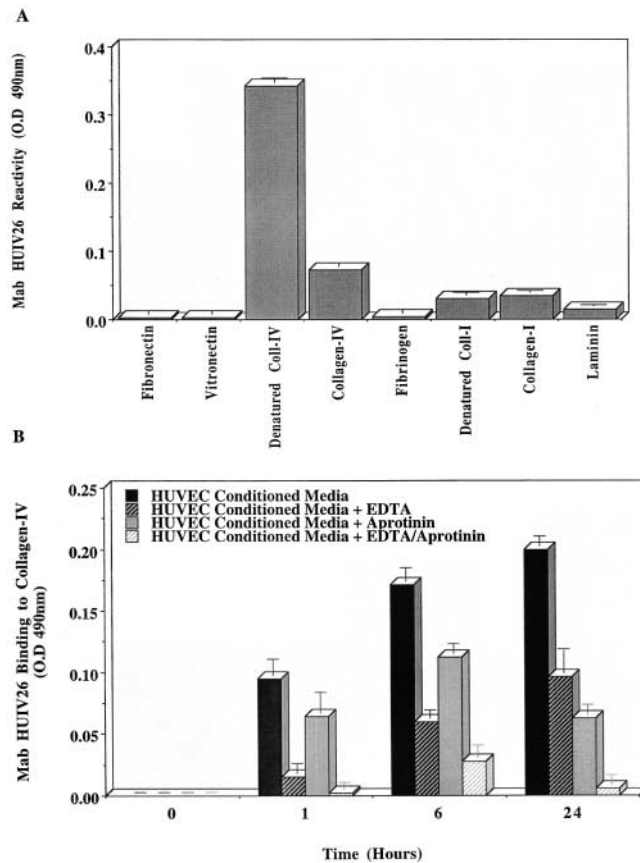Key words: angiogenesis; ECM; cryptic sites; tumor; migration

A

B

Figure 1. **Mab HUIV26 reactivity with denatured/proteolyzed collagen IV in solid phase ELISA.** Microtiter plates were coated with ECM components at a concentration of 25 μg/ml. (A) Mab HUIV26 was added (1 μg/ml), followed 1 h later with goat anti–mouse peroxidase–labeled IgG. All data was corrected for nonspecific binding of secondary antibody. Data bars represent the mean OD ± standard deviations from triplicate wells. (B) Microtiter wells were coated with triple helical collagen IV at 25 μg/ml. Concentrated (20×) HUVEC serum–free–conditioned media was added to the wells in the presence or absence of EDTA, aprotinin, or both and allowed to incubate for 1, 6, and 24 h. The plates were next washed, blocked, and incubated with Mab HUIV26 or control antibody. All data was corrected for nonspecific secondary antibody binding. Data bars represent the mean OD ± standard deviations from triplicate wells.

shown to be specifically exposed within the subendothelial basement membrane of angiogenic blood vessels, whereas little if any was detected in association with quiescent vessels. Importantly, our studies provide evidence that proteolytic exposure of this cryptic site within collagen IV plays a functional role in angiogenesis. In fact, a Mab HUIV26 directed to this cryptic site potently inhibited angiogenesis and tumor growth in multiple animal models. Together, these studies suggest a novel mechanism by which proteolytic remodeling of the ECM exposes cryptic protein sequences that promote novel integrin–ligand interactions required for angiogenesis in vivo.

Results

Mab HUIV26 binds to a cryptic site within collagen IV

We sought to generate a Mab that would specifically recognize proteolyzed or denatured collagen IV, but would not recognize triple helical collagen IV. To produce this antibody, we used the technique of subtractive immunization in conjunction with pepsin-solubilized human collagen IV (Xu et al., 2000). Although pepsin-solubilized collagen IV is not completely representative of native collagen IV found in vivo, it does retain most of its triple helical structure. As shown in Fig. 1 A, Mab HUIV26 specifically reacts with thermally denatured collagen IV, while showing little if any reactivity to triple helical collagen IV. Mab HUIV26 showed no reactivity to other ECM components, including fibronectin, laminin, vitronectin, or fibrinogen. Importantly, Mab HUIV26 was shown to react with a cryptic site within collagen type IV from a variety of species, including human, mouse, chick, and rat (Xu et al., 2000). Moreover, Mab HUIV26 did not react with denatured forms of collagen I or the triple helical or denatured forms of other collagens, including types II, III, or V (Xu et al., 2000).

Since angiogenesis is thought to be associated with proteolytic remodeling, we examined whether matrix-degrading enzymes had the capacity to expose the HUIV26 cryptic epitope. Microtiter wells were coated with triple helical collagen IV. Concentrated conditioned medium from human umbilical vein endothelial cells (HUVECs), which contains a variety of matrix-degrading enzymes, were added to the wells. As shown in Fig. 1 B, HUVEC-conditioned medium caused a time-dependent exposure of the HUIV26 cryptic epitope. Importantly, incubation in the presence of the metalloproteinase inhibitor EDTA significantly inhibited the exposure of the HUIV26 cryptic site. Moreover, addition of exogenous, naturally occurring matrix metalloproteinase (MMP) inhibitor TIMP-2 to the HUVEC condition medium also reduced the exposure of the HUIV26 cryptic site by ~30% (data not shown). Importantly, Mab HUIV26 does not react with any protein in the conditioned medium, thus demonstrating the specificity of the results. Interestingly, our recent studies involving retinal neovascularization in MMP-9–deficient mice revealed an ~70–80% reduction in the number of HUIV26 cryptic sites exposed per retina, as compared with control wild-type mice (unpublished data). Together, these findings provide evidence for a role for MMPs in the exposure of the HUIV26 cryptic epitope. The serine protease inhibitor aprotinin also reduced the exposure of the cryptic epitope but was more effective at later time points. However, a combination of both EDTA and aprotinin caused a near complete inhibition of the exposure of the HUIV26 cryptic site. Together, these findings suggest that the HUIV26 cryptic site can be exposed by proteolytic activity, which may include contributions from both MMPs and serine proteases.

Exposure of the HUIV26 cryptic site within the subendothelial basement membranes of angiogenic blood vessels

We assessed whether the HUIV26 cryptic epitope could be exposed within the basal lamina of blood vessels in vivo. Unfixed biopsy sections from normal human skin were incubated with either activated or proMMP-2, HT1080 tumor–conditioned medium, or control buffer. The tissues were costained with Mab HUIV26 (green) and a polyclonal antibody directed to factor VIII–related antigen (red), a known
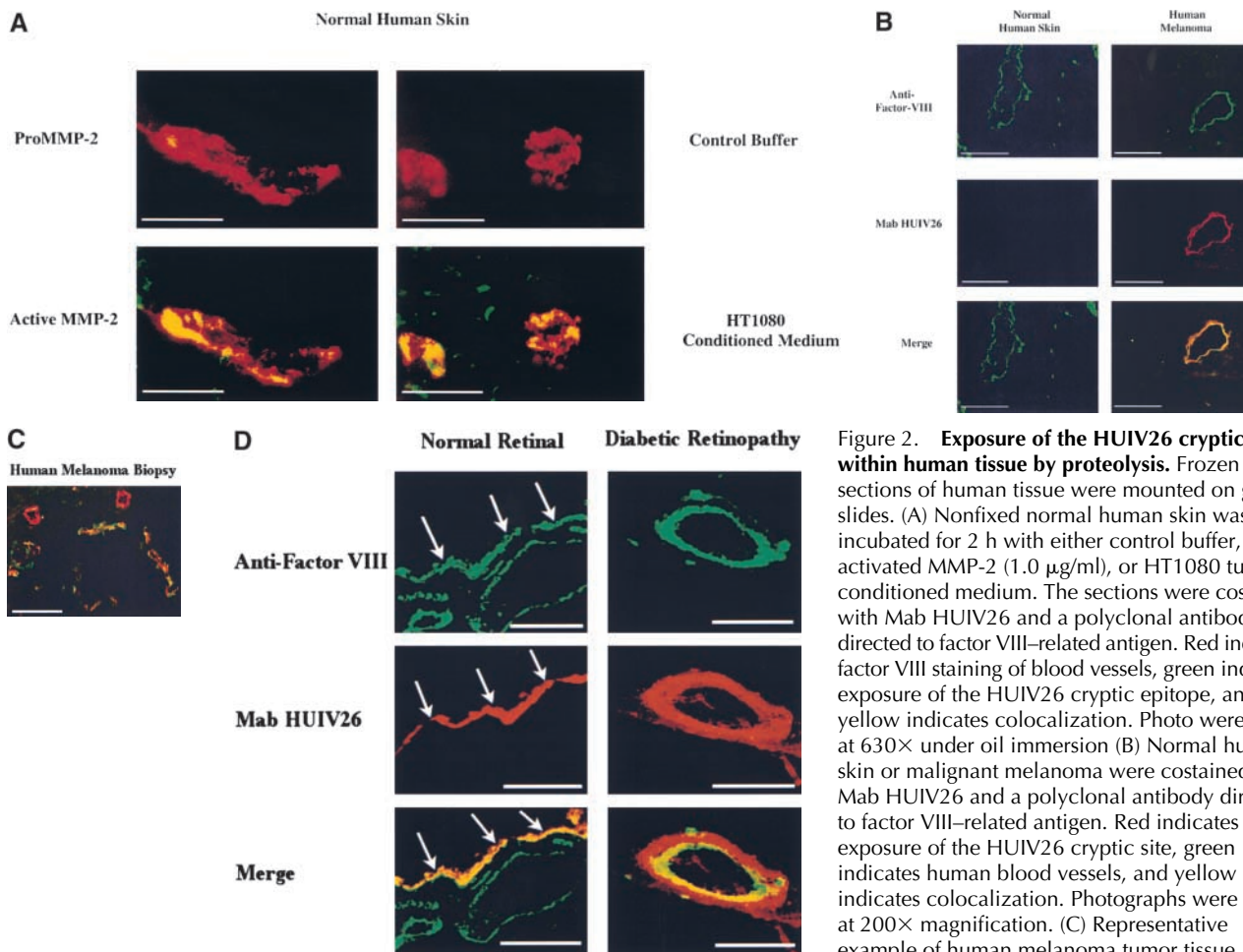
Figure 2. **Exposure of the HUIV26 cryptic site within human tissue by proteolysis.** Frozen sections of human tissue were mounted on glass slides. (A) Nonfixed normal human skin was incubated for 2 h with either control buffer, pro or activated MMP-2 (1.0 μg/ml), or HT1080 tumor–conditioned medium. The sections were costained with Mab HUIV26 and a polyclonal antibody directed to factor VIII–related antigen. Red indicates factor VIII staining of blood vessels, green indicates exposure of the HUIV26 cryptic epitope, and yellow indicates colocalization. Photo were taken at 630× under oil immersion (B) Normal human skin or malignant melanoma were costained with Mab HUIV26 and a polyclonal antibody directed to factor VIII–related antigen. Red indicates exposure of the HUIV26 cryptic site, green indicates human blood vessels, and yellow indicates colocalization. Photographs were taken at 200× magnification. (C) Representative example of human melanoma tumor tissue costained with Mab HUIV26 (green) and polyclonal antibody directed to factor VIII–related antigen (red), indicating that not all tumor vessels stain positive for HUIV26 epitope. Photos were taken at low power (200×). (D) Normal human retinal tissue or retina from subjects with diabetic retinopathy were costained with Mab HUIV26 and a polyclonal antibody to factor VIII–related antigen. Green indicates human blood vessels and red indicates HUIV26 cryptic sites. Arrows indicate nonspecific fluorescence of retinal pigmented epithelium due to auto-fluorescence of lipofusion. Photomicrographs were taken at 200× magnification. Bars, 50.0 μm.

marker of blood vessels. As shown in Fig. 2 A, blood vessels (red) from normal human skin were readily detected. Little if any of the cryptic HUIV26 epitope (green) was detected within the vascular basement membranes or the surrounding interstitial matrix from tissues treated with either inactive proMMP-2 or control buffer (Fig. 2 A, top). In contrast, tissues treated with either proteolytically active MMP-2 (Fig. 2 A, bottom left) or HT1080 tumor–conditioned medium (Fig. 2 A, bottom right) demonstrated exposure of the HUIV26 cryptic epitope, as indicated by colocalization (yellow) due to overlap of the exposed HUIV26 epitope (green) and factor VIII–related antigen (red). Together, these findings provide further evidence that the HUIV26 cryptic sites could be exposed by proteolytic activity in a physiological tissue.

To determine whether the HUIV26 cryptic site could also be exposed during invasive cellular processes such as angiogenesis and tumor growth in vivo, we examined biopsies from normal human skin and malignant melanoma. As shown in Fig. 2 B, left, blood vessels from normal human skin showed little if any exposure of the HUIV26 cryptic epitope (red). In contrast, the subendothelial basement

membrane of melanoma-associated (right) blood vessels showed extensive expression of the HUIV26 cryptic site (red). To estimate the relative percentage of tumor blood vessels that were associated with the HUIV26 cryptic epitope, costaining analysis for the expression of HUIV26 (red) and factor VIII–related antigen (green) was performed on a series of five melanoma tumor specimens. As shown in Fig. 2 C, although the HUIV26 cryptic epitope was detected in association with numerous blood vessels, not all vessels within a given field exhibited significant exposure of the HUIV26 epitope. In fact, analysis of these tissue sections revealed that an average of ∼66% of the tumor-associated vessels in any given field stained positive for the HUIV26 epitope (Table I). In similar experiments, we compared the blood vessels from normal human retina to retinas from patients with diabetic retinopathy. As shown in Fig. 2 D, left, normal retinal vessels showed little if any evidence of the HUIV26 cryptic epitope. However, nonspecific auto fluorescence from lipofucision (arrows) was detected within retinal-pigmented epithelium (RPE), as has been described in previous studies (Friedlander et al., 1996). In contrast, exposure of the HUIV26 cryptic epitope (red) was readily de-

Table I. **Expression of HUIV26 cryptic epitope in human melanoma vasculature**

Tumor specimen number	Vessels positive for HUIV26
	%
1	64
2	74
3	50
4	78
5	65

10 (200×) microscopic fields were examined for each melanoma tumor specimen. The percentage of HUIV26 staining vessels was estimated by dividing by the total number of vessels per field that stained positive for HUIV26 antigen and factor VIII–related antigen by the total number of vessels per field (factor VIII–related antigen positive).

tected within the subendothelial basement membrane of angiogenic retinal blood vessels from patients with diabetic retinopathy. Similar analysis of normal breast and bladder tissue showed little if any evidence of the HUIV26 cryptic site, whereas the subendothelial basement membranes of blood vessels from both human breast and bladder tumors stained positive (data not shown). Together, these results suggest that the HUIV26 cryptic epitope may be an important marker of angiogenic blood vessels in vivo.

Exposure of the HUIV26 cryptic epitope correlates with the expression and conversion of pro-MMP-2 to active MMP-2 in vivo

Our previous studies indicated that incubation of normal human tissue with proteolytically active MMP-2, but not inactive pro-MMP-2, can expose the HUIV26 cryptic site in situ. Therefore, we examined whether the expression of MMP-2 was associated with the exposure of the HUIV26 epitope during angiogenesis in vivo. To facilitate these studies, angiogenesis was induced within the chick chorioallantoic membrane (CAM) by either purified bFGF or a single cell suspension of CS1 melanoma cells. CAM tissues were costained with either Mab HUIV26 or a polyclonal antibody to MMP-2, or a polyclonal antibody directed to factor VIII–related antigen. As shown in Fig. 3 A, top, MMP-2 (red) colocalized (yellow) with the cryptic HUIV26 epitope (green) in blood vessels from either cytokine- or tumor-induced angiogenesis. To confirm the exposure of the HUIV26 cryptic epitope within the basement membrane of blood vessels, similar CAM tissues were costained with polyclonal antibody directed to factor VIII–related antigen and Mab HUIV26. As shown in Fig. 3 A, bottom, the HUIV26 cryptic epitope was associated with both bFGF-induced and tumor-induced angiogenic blood vessels. To determine
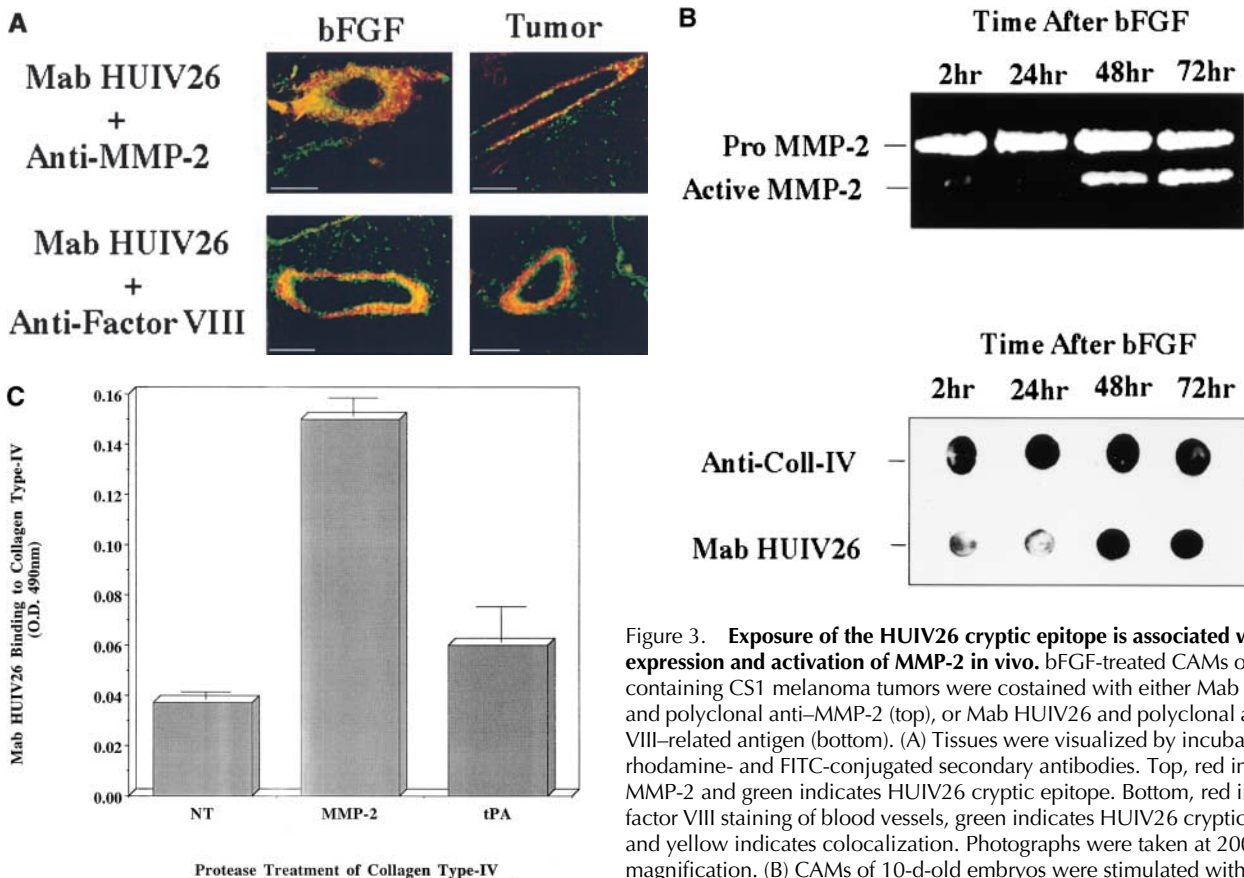

Figure 3. **Exposure of the HUIV26 cryptic epitope is associated with the expression and activation of MMP-2 in vivo.** bFGF-treated CAMs or CAMs containing CS1 melanoma tumors were costained with either Mab HUIV26 and polyclonal anti–MMP-2 (top), or Mab HUIV26 and polyclonal antifactor VIII–related antigen (bottom). (A) Tissues were visualized by incubation with rhodamine- and FITC-conjugated secondary antibodies. Top, red indicates MMP-2 and green indicates HUIV26 cryptic epitope. Bottom, red indicates factor VIII staining of blood vessels, green indicates HUIV26 cryptic epitope, and yellow indicates colocalization. Photographs were taken at 200× magnification. (B) CAMs of 10-d-old embryos were stimulated with bFGF and total CAM lysates were prepared at 2, 24, 48, and 72 h. Top, gelatin zymogram of total CAM lysates after stimulation with bFGF. Bottom, dot blot of total CAM lysates. Total collagen IV (triple helical and denatured) was detected with a polyclonal antibody to both native and denatured collagen IV. Denatured collagen IV was detected with Mab HUIV26. (C) Microtiter plates were coated with triple helical collagen type IV (25 μg/ml). MMP-2 (500 ng/ml), tPA (6 U/ml, specific activity 700 μg/mg protein), or NT (control buffer) were incubated for 18 h. The wells were washed, blocked with BSA, and the HUIV26 cryptic sites were detected with Mab HUIV26 (1.0 μg/ml). Data bars represent the mean OD ± standard deviations from triplicate wells. Bars, 50.0 μm.
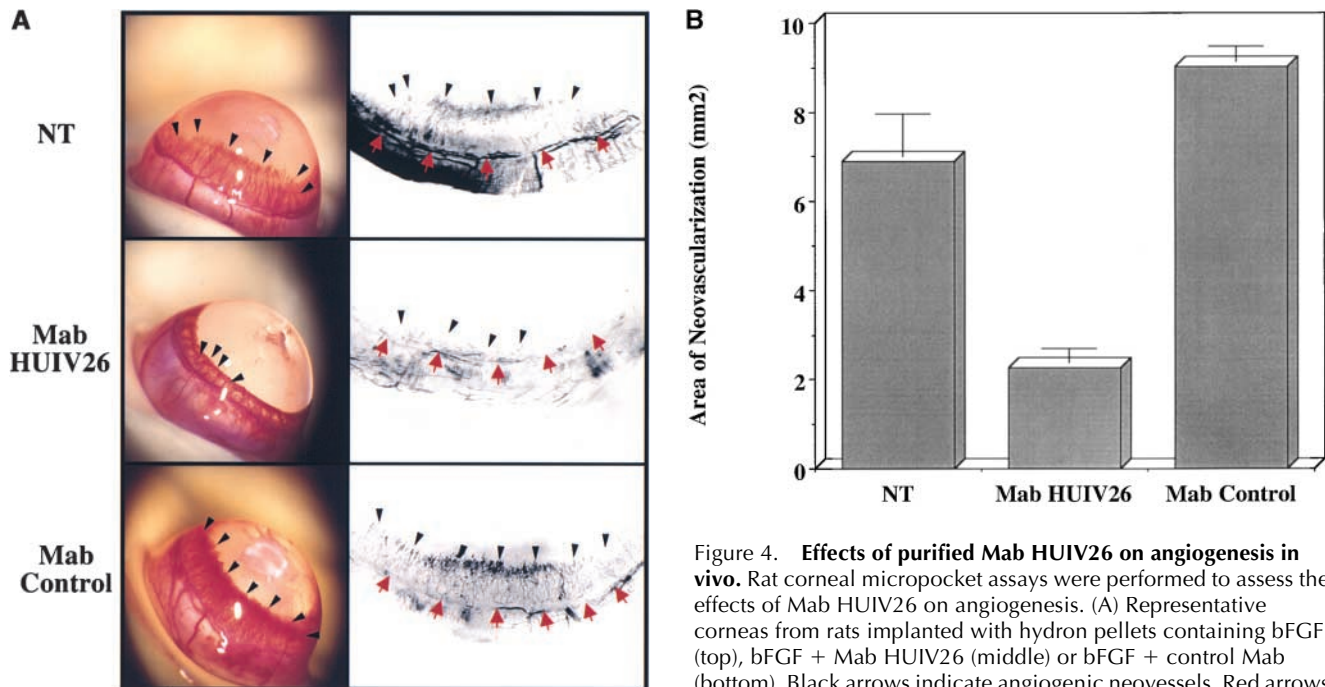
Figure 4. **Effects of purified Mab HUIV26 on angiogenesis in vivo.** Rat corneal micropocket assays were performed to assess the effects of Mab HUIV26 on angiogenesis. (A) Representative corneas from rats implanted with hydron pellets containing bFGF (top), bFGF + Mab HUIV26 (middle) or bFGF + control Mab (bottom). Black arrows indicate angiogenic neovessels. Red arrows indicate preexisting limbal vessels. (B) Quantification of the area of neovascularization within rat corneas. Data bars represent the mean area of neovascularization from the limbus to hydron pellet. Experiments were performed at least twice with five to seven eyes per condition.

whether the proteolytically active form of MMP-2 correlated with exposure of the HUIV26 cryptic epitope, tissue lysates were prepared from these CAMs after bFGF stimulation and analyzed by both gelatin zymography and dot blot analysis. As shown in Fig. 3 B, top, bFGF treatment was associated with a time-dependent conversion of the latent 72-kD MMP-2 to its proteolytically active 62-kD species between 24 and 48 h after stimulation. These findings were consistent with our previously published results (Brooks et al., 1996). The gelatinolytic bands were confirmed to be pro (72 kD) and active (62 kD) MMP-2 by Western blot analysis (data not shown). Interestingly, dot blot analysis of these same lysates demonstrated the generation of the HUIV26 epitope between 24 and 48 h which correlated directly with the bFGF-associated activation of MMP-2. To confirm that activated MMP-2 can contribute to the exposure of the HUIV26 epitope, in vitro ELISA assays were conducted. Triple helical collagen type IV was coated on microtiter wells as described above. The wells were next incubated with either activated MMP-2, the serine protease tPA, or control buffer for 18 h. The wells were washed and the HUIV26 cryptic epitope was detected with Mab HUIV26. As shown in Fig. 3 C, incubation of triple helical collagen type IV with activated MMP-2 caused an approximately threefold increase in the exposure of the HUIV26 epitope as compared with either no treatment (control buffer), or the serine protease tPA. These findings provide further evidence that MMPs such as MMP-2 may contribute to the exposure of the HUIV26 epitope. However, these results do not rule out the likely contributions of other MMPs or serine proteases in the exposure of the HUIV26 cryptic site in vivo. Since MMP-9, the second major MMP capable of cleaving triple helical collagen IV, was not detected in the CAM lysates,

it is likely, but not direct proof, that MMP-2 is at least one protease that may contribute to the generation of the HUIV26 epitope in the chick embryo model.

Mab HUIV26 potently inhibits angiogenesis in vivo

Previous studies indicated that MMP-2–mediated proteolysis of collagen IV within the basement membrane preparation Matrigel resulted in enhanced endothelial cord formation (Schnaper et al., 1993). Moreover, our studies indicate that the HUIV26 cryptic site can be exposed after thermal denaturation of Matrigel (data not shown). Together, these findings suggest that cellular interactions with the HUIV26 cryptic epitope may facilitate angiogenesis. To examine this possibility, we analyzed the effects of Mab HUIV26 in the rat corneal micropocket assay (Dipietro et al., 1998). Hydron pellets containing either bFGF alone, bFGF plus HUIV26, or bFGF plus an isotype-matched control antibody were surgically implanted into the corneas of rats (Dipietro et al., 1998). After a 5-d incubation period, corneal angiogenesis was quantified (Koch et al., 1995). As shown in Fig. 4 A, bFGF induced a strong angiogenic response in the rat corneas (top). In contrast, little angiogenesis was detected in the corneas implanted with bFGF hydron pellets containing Mab HUIV26 (middle), as compared with either no treatment or treated with an isotype-matched control antibody (top and bottom). In fact, as shown in Fig. 4 B, rat corneal angiogenesis was inhibited by >70% as compared with controls ($P < 0.001$). Similar results were observed with bFGF- or VEGF-induced angiogenesis within the chick CAM model (data not shown). These findings provide evidence for a potent inhibitory activity for Mab HUIV26 on cytokine-induced angiogenesis in vivo.
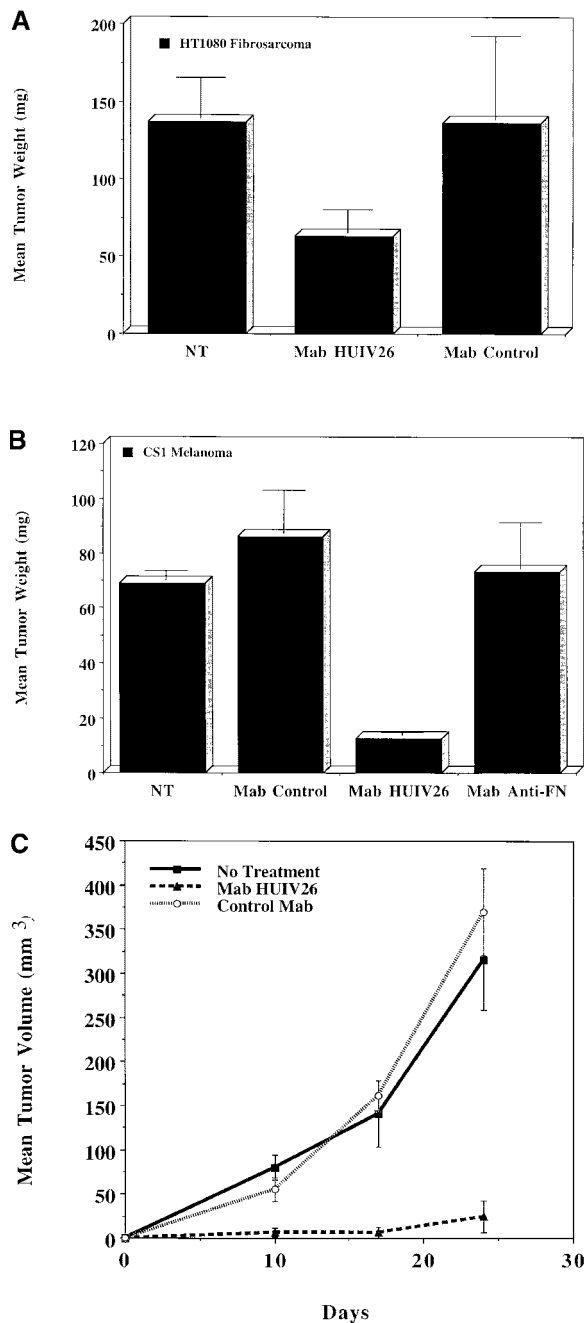
Figure 5. **Effects of systemic administration of purified Mab HUIV26 on tumor growth in vivo.** The effects of Mab HUIV26 on tumor growth was assessed in two independent models, including the chick embryo (A and B) and the SCID Mouse (C). HT1080 human fibrosarcoma cells (4×10^5) or CS-1 melanoma tumor cells (5×10^6) were inoculated on the CAMs of 10-d-old chick embryos. 24 h later, the embryos received a single intravenous injection of 100 μg of Mab HUIV26 or isotype-matched control. (A) Quantitation of HT1080 tumor growth in the chick embryo. (B) Quantitation of CS-1 tumor growth within the chick embryo. Data bars represent the mean tumor weights ± the standard errors from 5 to 10 embryos per condition. (C) SCID mice were injected subcutaneously with 2×10^6 M21 human melanoma cells. 3 d later mice were treated i.p. daily for 24 d with 100 μg of either Mab HUIV26 or an isotype-matched control antibody. Tumor size was monitored with calipers and tumor volumes were determined. Data represents the mean ± standard errors of the tumor volumes. All experiments were conducted 3 to 4 times with 5 to 10 animals per condition.

Systemic administration of Mab HUIV26 potently inhibits tumor growth in vivo

The growth of most all solid tumors is thought to depend on angiogenesis (Weidner et al., 1991, 1992). Therefore, we evaluated its effects on the growth of tumors of distinct histological origin within two independent animal models. First, CS1 melanoma or HT1080 human fibrosarcoma cells were applied to the CAMs of 10-d-old chick embryos (Brooks et al., 1996). 24 h latter, the embryos were treated systemically with a single injection (100 μg/embryo) of either Mab HUIV26 or an isotype-matched control antibody. As shown in Fig. 5, A and B, Mab HUIV26 inhibited HT1080 and CS1 tumor growth by 50 and 80%, respectively. Treatment of these embryos with either an irrelevant isotype-matched control antibody or an antibody directed to the ECM protein fibronectin showed little if any effect.

To confirm these findings in a second animal model, we examined the effects of Mab HUIV26 on M21 human melanoma tumor growth in severe combined immunodeficient (SCID) mice. M21 human melanoma cells (2×10^6) were injected subcutaneously in SCID mice. 3 d later the mice were treated with daily i.p. injections of either Mab HUIV26 or isotype-matched control antibody (100 μg/ mouse). As shown in Fig. 5 C, mice from either untreated or treated with an irrelevant isotype-matched control antibody formed tumors of similar size. In contrast, M21 tumor growth in mice treated with Mab HUIV26 were inhibited by 80 to 90% as compared with controls. These findings confirm the potent antitumor activity of Mab HUIV26 and demonstrate that this activity is not limited to a single tumor type or animal model.

Mab HUIV26 inhibits human endothelial cell adhesion and migration on denatured, but not triple helical, collagen IV

It is possible that exposure of the HUIV26 cryptic epitope may contribute to angiogenesis in part by regulating endothelial cell–integrin interactions. To examine this possibility, we evaluated the effects of Mab HUIV26 on human endothelial cell adhesion to either triple helical or denatured human collagen IV. HUVECs were allowed to attach to immobilized triple helical or denatured collagen IV in the presence or absence of Mab HUIV26 or isotype-matched control antibody (50 μg/ml). As shown if Fig. 6 A, HUVECs readily attached to both triple helical and denatured collagen IV. In contrast, HUVEC adhesion to denatured collagen IV was inhibited by ∼60% in the presence of Mab HUIV26, while having little if any effect on adhesion to triple helical collagen IV. An isotype-matched control antibody had no effect of cell adhesion to either triple helical or denatured collagen IV.

In similar experiments, we examined the effects of Mab HUIV26 on HUVEC migration in vitro. Membranes from Transwell™ migration chambers were coated with either triple helical or denatured collagen IV. HUVECs were resuspended in migration buffer in the presence or absence of Mab HUIV26 or an isotype-matched control antibody (50 μg/ml). As shown in Fig. 6 B, Mab HUIV26 had little if
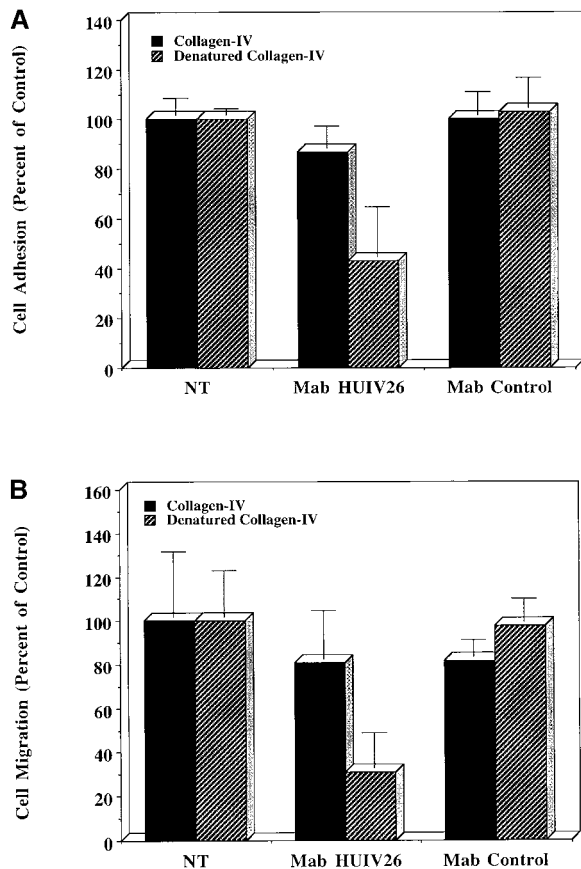
Figure 6. **Effects of Mab HUIV26 on human endothelial cell adhesion and migration.** Microtiter plates (96 wells) and Transwell membranes were coated with triple helical or denatured collagen type IV (25 μg/ml). (A) Subconfluent HUVECs (10^5) were resuspended in adhesion buffer and allowed to attach in the presence or absence of Mab HUIV26 or an isotype-matched control antibody for 30 min. Nonattached cells were removed by washing and the attached cells were stained with crystal violet. (B) Subconfluent HUVECs (10^5) were resuspended in migration buffer and allowed to migrate in the presence or absence of Mab HUIV26 or an isotype-matched control antibody. Cells remaining on the top side of the membrane were removed and cells that had migrated to the under side were stained with crystal violet. Cell adhesion and migration was quantified by measuring the OD of eluted dye at 600 nm. Data bars represent the mean OD ± standard deviation from triplicate wells expressed as a percentage of control.

any effect on HUVEC migration or triple helical collagen, but inhibited migration by ∼70% on denatured collagen IV. HUVEC migration was not effected by an isotype-matched control antibody. These findings suggest a potential mechanism by which Mab HUIV26 may disrupt angiogenesis by inhibiting endothelial cell interactions with the HUIV26 cryptic epitope, thereby disrupting adhesion and migration.

Mab HUIV26 inhibits purified integrin αvβ3 binding to denatured collagen IV

We sought to determine whether an integrin receptor was involved in mediating cellular interactions with the HUIV26 cryptic epitope. To facilitate these studies, microtiter wells were coated with either triple helical or denatured

collagen IV. The wells were incubated with purified integrin receptors, including α1β1, α2β1, αvβ3, and α5β1. After incubation, bound integrins were detected with antiintegrin-specific antibodies. As shown in Fig. 7 A, the collagen-binding integrins α1β1 and α2β1 bound to triple helical collagen in a dose-responsive manner, whereas integrins αvβ3 and α5β1 showed little if any interaction. After denaturation, α1β1 binding was lost; however, denatured collagen IV acquired the capacity to bind to integrin αvβ3 (Fig. 7 B). Moreover, denatured collagen IV retained its ability to bind to α2β1, whereas the control fibronectin receptor integrin α5β1 failed to interact (Fig. 7 B). These findings suggest that denaturation of the triple helical structure of collagen IV can shift integrin binding specificity from that of a β1 dependency to both β1 and αvβ3. To determine whether integrin α2β1 or integrin αvβ3 interacts with the HUIV26 cryptic epitope, similar receptor binding assays were performed in the presence or absence of Mab HUIV26 or an isotype-matched control antibody. As shown in Fig. 7 C, Mab HUIV26 failed to block the ability of purified integrin α2β1 to bind to denatured collagen IV, while inhibiting integrin αvβ3 binding by >70%. Together, these findings suggest that integrin αvβ3 may function as a receptor for the HUIV26 cryptic epitope.

It is known that the tripeptide sequence RGD is recognized by integrin αvβ3 (Smith and Cheresh, 1988). Collagen IV has 11 different RGD-containing sites, which appear to be cryptic since integrin αvβ3 fails to bind to triple helical collagen IV. Therefore, it is possible that one or more of these RGD sequences may represent the HUIV26 cryptic epitope. To examine this possibility, we synthesized 10-mer peptides corresponding to all 11 distinct RGD sites within collagen IV. Integrin αvβ3 could bind to all 11 RGD peptides, yet none of the RGD peptides were recognized by Mab HUIV26. Moreover, none of the 11 peptides were capable of blocking Mab HUIV26 binding to denatured collagen IV (data not shown). Although these findings do not completely rule out the possibility that an RGD sequence is associated with the HUIV26 cryptic site, they do suggest that RGD sequences within collagen IV are not sufficient to support interactions with Mab HUIV26 and that other protein sequences are critical for Mab HUIV26 recognition of its epitope. Further studies are now under way to more precisely identify the amino acid sequence of the HUIV26 cryptic site.

Discussion

Angiogenesis plays a critical role in the normal development as well as the spread of tumors to distant sites (Risau and Lemmon, 1988; Brooks et al., 1994; Hanahan and Folkman, 1996). Several elegant studies have demonstrated the importance of numerous families of molecules in the regulation of angiogenesis (Blood and Zetter, 1990; Rak et al., 1995; Suri et al., 1996). The majority of these studies have focused on growth factors and their receptors, cell adhesion molecules, and matrix-degrading proteases (Liotta et al., 1991; O'Reilly et al., 1994; Brooks et al., 1996; Vu et al., 1998). In comparison, relatively little emphasis has been placed on the ECM as a potential therapeutic target to regulate neovascularization.
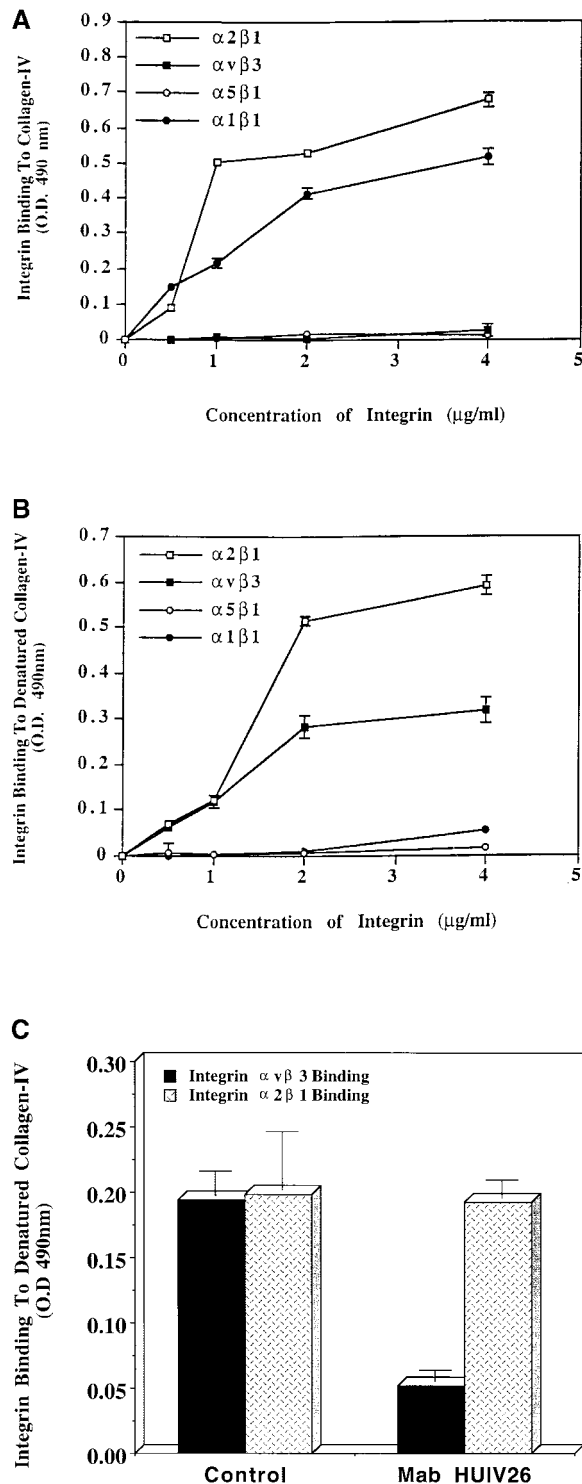
Figure 7. **Integrin binding to triple helical and denatured human collagen IV.** Microtiter wells were coated with either triple helical or denatured human collagen IV (25 μg/ml). Purified human integrins α1β1, α2β1, α5β1, or αvβ3 (0.5–4 μg/ml) were allowed to bind to triple helical collagen IV (A) or denatured collagen IV (B) for 1 h at 37°C. Integrin binding was detected with antiintegrin antibodies. (C) Purified human integrins α2β1 and αvβ3 (1.0 μg/ml) were allowed to bind to denatured collagen IV–coated plates for 1 h at 37°C in the presence or absence of Mab HUIV26 or an isotype-matched control antibody. Integrin binding was detected by incubation with either polyclonal antibody directed to α2 or α3 integrins. Data bars represent the mean OD ± standard deviations from triplicate wells.

Recent studies have indicated that proteolytic enzymes, such as members of the MMP family, play an important role in angiogenesis (Hiraoka et al., 1998; Stetler-Stevenson, 1999; Werb et al., 1999). In fact, mice deficient in MMP-2 or MMP-9 exhibit reduced angiogenesis in vivo (Itoh et al., 1998; Vu et al., 1998). Moreover, our recent studies suggest that MMP-9–deficient mice exhibit reduced exposure of the HUIV26 sites within the retina during hypoxia-induced retinal neovascularization in vivo (unpublished data). Together, these findings suggest that proteolysis of collagen, as well as perhaps other ECM proteins, is of critical importance in angiogenesis. Although soluble fragments of collagen have been detected in the circulation, little if any direct evidence is available that proteolyzed matrix–associated forms of collagen IV exist within the subendothelial basement membrane or that they play a functional role in angiogenesis (Jukkola et al., 1997). Here, we describe the use of a unique Mab that specifically binds to proteolyzed and denatured collagen IV, but does not react with triple helical collagen IV. This cryptic HUIV26 epitope was shown to be specifically exposed within the subendothelial basement membrane of angiogenic and tumor-associated blood vessels, but not within the basement membrane of normal vessels. The high degree of specificity for angiogenic and tumor vessels is likely due to the slow turnover of members of the collagen family in healthy tissues as compared with the rapid remodeling that likely occurs during angiogenesis.

Recent evidence suggests that cellular interactions with proteolyzed forms of ECM molecules such as osteopontin, and laminin may result in altered cellular behavior including changes in cell motility (Senger and Perruzzi, 1996; Giannelli et al., 1997; Davis et al., 2000). Thus, proteolytic cleavage of ECM proteins, together with cell surface receptor binding events, may represent a previously unappreciated mechanism to transmit cryptic regulatory signals that are required for angiogenesis. Consistent with this hypothesis, we provide evidence that a Mab directed to the matrix-immobilized HUIV26 cryptic site potently inhibits angiogenesis in multiple animal models. Importantly, angiogenesis was inhibited irregardless of the cytokine used or the animal species in which these assays were conducted. Moreover, systemic administration of Mab HUIV26 also potently inhibited the growth of several tumor types of distinct histological origin. Interestingly, the exposure of the HUIV26 epitope was associated with a loss of α1β1 binding and a gain in αvβ3 binding, whereas α2β1-mediated interactions were unaffected. This shift in integrin binding may initiate a unique signaling cascade required for angiogenesis in vivo.

Importantly, recent studies have indicated that MMP-mediated cleavage of laminin 5 can expose a cryptic epitope which potentiates tumor cell motility in vitro (Giannelli et al., 1997). Moreover, proteolytic cleavage of fibronectin and osteopontin also enhance cellular migration in vitro (Bowersox and Sorgenete, 1982; Senger and Perruzzi, 1996). However, little is known concerning the roles that these proteolyzed ECM proteins may have on pathological processes in vivo. Here, we provide evidence for the first time that proteolytic exposure of the HUIV26 cryptic site is required for angiogenesis and tumor growth in vivo. Moreover, our results suggest that proteolytic remodeling is not solely a mechanism

to destroy physical barriers that obstruct vascular cell migration, but can expose cryptic sites that are essential for the angiogenic process. In fact, our systematic search for cryptic sites in other ECM proteins have resulted in the generation of several distinct Mab directed to different cryptic epitopes which potently inhibit angiogenesis and tumor growth (unpublished data). Thus, an in depth knowledge of the roles these cryptic sites play in angiogenesis is critical to our understanding of blood vessel formation. Together, our findings indicate that targeting matrix-immobilized cryptic sites within ECM molecules may be a highly specific and powerful new approach for the treatment of neoplastic diseases.

Materials and methods

Antibodies and reagents

Mab HUIV26 directed to a cryptic site within collagen IV was generated by subtractive immunization (Xu et al., 2000). The immunogen used for the production of Mab HUIV26 was thermally denatured, pepsin-solubilized human collagen IV from Sigma-Aldrich. Mab HUIV26 recognizes a cryptic epitope within collagen IV from a variety of species, including human, chick, rat, and mouse, but does not react with triple helical collagen IV. Mab LM609 (anti-$\alpha v \beta 3$) and vitronectin were gifts from Dr. David Cheresh (Scripps Research Institute, La Jolla, CA). Antifactor VIII–related antigen polyclonal antibody was obtained from BioGenex. Antifibronectin Mab and normal mouse isotype–matched control antibodies were obtained from Sigma-Aldrich. Mabs 1973 (anti-$\alpha 1$), 1950 (anti-$\alpha 2$), 1928 (anti-$\alpha 5$), and polyclonal antibodies AB769 (anticollagen IV) and AB809 (anti–MMP-2) were obtained from Chemicon International. FITC- and rhodamine-conjugated secondary antibodies were from BioSource International. Purified ECM molecules, fibronectin, laminin, fibrinogen, collagen I, and collagen IV were obtained from Sigma-Aldrich. Purified MMP-2 was obtained from Chemicon International. OCT-embedding compound was from VWR Scientific Products. Purified integrins $\alpha 1 \beta 1$, $\alpha v \beta 3$, and $\alpha 5 \beta 1$ were obtained from Chemicon International. Integrin $\alpha 2 \beta 1$ was purified from platelets as described previously (Davis, 1992).

Cells and cell culture

Human melanoma cell line M21 was a gift from Dr. David Cheresh (Scripps Research Institute, La Jolla, CA). CS1 hamster melanoma cells were provided by Dr. C. Damsky (University of California, San Francisco, CA). Human Fibrosarcoma cell line HT1080 was obtained from the American Type Culture Collection. Cell lines were maintained in RPMI 1640 supplemented with 10% FBS, 2 mM L-glutamine, and Pen-Strep. HUVECs were obtained from Clonectics Corp. and were maintained in M199 medium containing 20% FBS, 100 μg/ml gentamicin, 4 mM L-glutamine, 0.9 mg/ml heparin, and 30 μg/ml ECGS (Upstate Biotechnology).

Solid phase ELISA

Nontissue culture–treated 96-well ELISA plates were coated (50 μl/well) with ECM proteins (25 μg/ml in PBS) for 18 h at 4°C. Plates were blocked with 100 μl/well of 1.0% BSA in PBS for 1 h at 37°C. Purified Mab HUIV26 (1.0 μg/ml) was diluted in 1.0% BSA in PBS (100 μl/well). Plates were incubated for 1 h at 37°C and washed three times with PBS. Goat anti–mouse peroxidase–conjugated IgG was added and allowed to incubate for 1 h at 37°C. The plates were washed three times with PBS and ELISA substrate (OPD) was added and the OD was measured with an ELISA plate reader at a wavelength of 490 nm. All measurements were corrected for nonspecific binding to BSA and reactivity of secondary antibody.

For proteolyzed collagen IV ELISAs, microtiter plates were coated as described above with collagen IV. Concentrated (20×) HUVEC serum-free–conditioned medium (100 μl/well) with or without EDTA (50 mM) or aprotinin (10 μg/ml) was incubated for 1, 6, and 24 h at 37°C. At each time point, the wells were washed five times with PBS/EDTA and blocked with 1.0% BSA. No significant loss of total bound collagen IV was noted between experimental conditions, as detected by control incubations with polyclonal antibodies directed to collagen IV. Detection of Mab HUIV26 immunoreactivity was performed as described above.

Immunofluorescence analysis of tissue sections

Human and chick tissues were embedded in OCT and snap frozen in liquid nitrogen (Brooks et al., 1996). In brief, 4-um sections of normal human skin, retina, and chick CAM, or human malignant melanoma or retina from patients with diabetic retinopathy were fixed by incubation for 30 s in 50% methanol/50% acetone. Tissue were blocked by incubation with 2.5% BSA in PBS followed by incubation with primary antibodies HUIV26 (100 μg/ml), anti-MMP-2 (50 μg/ml), or polyclonal antifactor VIII (1:100 dilution) in 1.0% BSA in PBS for 2 h at 37°C. In control experiments, tissues were incubated with secondary antibodies only. Tissue were washed five times in PBS for 5 min each followed by incubation with FITC- and rhodamine-conjugated secondary antibodies (1:400 dilution in 1.0% BSA in PBS) for 1 h at 37°C. In experiments in which the tissues were proteolyzed before staining, unfixed frozen sections were incubated with either control buffer alone (50 mM Tris, 200 mM NaCl, 10 mM CaCl$_2$, pH 7.5), activated or Pro MMP-2 (1.0 μg/ml), or concentrated (20×) serum–free HT1080–conditioned medium for 2 h at 37°C. The tissues were then washed extensively five times with PBS. Costaining with primary antibodies was carried out as described above. Photomicrographs were taken at either low (200×) or high power (630×).

Quantitation of HUIV26-positive tumor blood vessels

To assess the relative percentage of HUIV26-positive tumor blood vessels, costain analysis was performed on frozen sections of human melanoma tumor biopsies. In brief, 4.0-um tissue sections were cut from frozen blocks of human malignant melanoma tumors. The tissues were costained with Mab HUIV26 and a polyclonal antibody directed to factor VIII–related antigen. 10 sections were analyzed for each of 5 distinct tumors. For each tumor, the percentage of HUIV26-positive vessels were estimated by determining the number of tumor vessels that costained for both HUIV26- and factor VIII–related antigen, as compared with the vessels that only stained positive for factor VIII–related antigen. These observations were conducted using low power magnification (200×).

Gelatin zymography and dot blot analysis

Angiogenesis was induced within the CAMs of 10-d-old chick embryos by placing a filter disc saturated with bFGF (25 μl) at 1.0 μg/ml (Brooks et al., 1998). Tissue directly beneath the filter discs were harvested at 2, 24, 48, and 72 h after addition of the bFGF. CAM tissues were homogenized in lysis buffer containing 1.0% TX-100, 50 mM Tris, 300 mM NaCl, pH 7.5. 20 μg of total CAM lysate were electrophoresed through a 10% SDS-PAGE gel polymerized with 0.2% gelatin (Brooks et al., 1996). Gels were washed three times for 1 h each with 2.5% TX-100 and incubated for 16 h at 37°C in collagenase buffer containing 50 mM TRIS, 200 mM NaCl, and 10 mM CaCl$_2$, pH 7.5. Gelatinolytic activity was visualized by staining with 0.5% Coomassie blue. Gelatinolytic bands were confirmed to be pro and active MMP-2 by Western blot analysis with anti-MMP-2–specific Mab.

In dot blot analysis, 10 μg of total protein was spotted (10 μl/spot) on nitrocellulose paper. Blots were incubated in 10% milk diluted in TBS-T to block nonspecific binding and incubated with either anticollagen IV polyclonal antibody or Mab HUIV26 (1.0 μg/ml). Blots were next washed and incubated with peroxidase-labeled secondary antibodies. Immunoreactive bands were visualized by enhanced chemiluminescence according to the manufacture's instructions.

Rat corneal micropocket angiogenesis assay

The rat corneal micropocket angiogenesis assay was performed essentially as described (Koch et al., 1995; Dipietro et al., 1998). In brief, hydron pellets (Polyhydroxyethyl methacrylate; Interferon Sciences) were prepared containing 1.2 μl of saline, 1.2 μl of bFGF, either Mab HUIV26 or control Ab (50 μg), and 12 μl of 12% hydron in ethanol. Mixtures were applied to a 1.5-mm diameter Teflon rod (Dupont). The hydron pellets were dried in a laminar flow hood. Pockets were cut in the corneal stroma of F344 female rats, 1.5-mm from the limbus and the Hydron pellets implanted (Koch et al., 1995; Dipietro et al., 1998). Corneas were routinely examined by slit-lamp biomicroscopy for up to 5 d. Corneas were photographed on day 5 after implantation. Rats were anesthetized and perfused with saline followed by colloidal carbon to enhance visualization of blood vessels. The corneas were dissected, fixed in 4% paraformaldehyde, and mounted on glass slides in 50% glycerol/50% gelatin solution. Corneal neovascularization was quantified by measuring the area of neovascularization from the limbus to the pellet. The area of neovascularization was acquired with Image Pro Plus 3.0 software (Media Cybernetics). Experiments were conducted two to three times with five to seven eyes per condition.

Chick embryo tumor growth assays

Single cell suspensions of CS1 melanoma (5×10^6 per embryo) or HT1080 fibrosarcoma (4×10^5 per embryo) were applied in a total volume of 40 μl of RPMI to the CAMs of 10-d-old embryos (Brooks et al., 1998). 24 h later,

the embryos received a single intravenous injection of purified Mabs HUIV26 or control Mabs (100 μg per embryo). Tumors were grown for 7 d, then resected and wet weights were determined. Experiments were performed three to four times with five to ten embryos per condition.

SCID mouse tumor growth assay

Subconfluent human M21 melanoma cells were harvested, washed, and resuspended in sterile PBS (20×10^6 per ml). SCID mice were injected subcutaneously with 100 μl of M21 human melanoma cell (2×10^6) suspension. 3 d after tumor cell injection, mice were either untreated or treated i.p. (100 μg/ mouse) with either Mab HUIV26 or an isotype-matched control antibody. The mice were treated daily for 24 d. Tumor size was measured with calipers and the volume was estimated using the formula $V = L^2 \times W/2$, where V is equal to the volume, L is equal to the length, and W is equal to the width. Experiments were completed three times with similar results

Cell adhesion assays

Human collagen type IV (triple helical or denatured) was immobilized (25 μg/ml) on 48-well nontissue culture–treated plates. Wells were washed and incubated with 1% BSA in PBS for 1 h at 37°C. Subconfluent HUVECs were harvested, washed, and resuspended in adhesion buffer containing RPMI 1640, 1 mM $MgCl_2$, 0.2 mM $MnCl_2$, and 0.5% BSA. HUVECs (10^5) were resuspended in 200 μl of the adhesion buffer in the presence or absence of Mab HUIV26 or control antibodies (50 μg/ml) and were added to each well and allowed to attach for 30 min at 37°C. The nonattached cells were removed and the attached cells were stained for 10 min with crystal violet as described (Petitclerc et al., 1999). The wells were washed three times with PBS and cell-associated crystal violet was eluted by addition of 100 μl of 10% acetic acid. Cell adhesion was quantified by measuring the optical density of eluted crystal violet at a wavelength of 600 nm.

Cell migration assays

Transwells membranes (8.0-μm pore size) were coated with human collagen type IV (triple helical or denatured) for 16 h at 4°C. Next, 600 μl of migration buffer (RPMI 1640, 1 mM $MgCl_2$, 0.2 mM $MnCl_2$, and 0.5% BSA) was added to the lower chamber. HUVECs (10^5) were resuspended in migration buffer in the presence or absence of Mab HUIV26 or control antibodies (50 μg/ml) and added to upper chamber and allowed to migrate for 5 h at 37°C. Cells remaining on the top of the membrane were removed and cells that had migrated to the underside were fixed and stained with crystal violet. The membranes were washed and the cell-associated crystal violet was eluted with 10% acetic acid. Cell migration was quantified by measuring the optical density of eluted crystal violet at a wavelength of 600 nm.

Purified integrin receptor binding assays

ELISA plates (96 well) were coated with either 25 μg/ml of denatured or triple helical collagen IV for 18 h at 4°C. Plates were washed three times with 200 μl of PBS and blocked with 100 μl/well of 1.0% BSA in PBS for 1 h at 37°C. Purified human integrin receptors (α1β1, α2β1, α5β1, and αvβ3) were diluted in binding buffer containing 20 mM Tris, 150 mM NaCl, 1 mM $MgCl_2$, 0.2 mM $MnCl_2$, 0.5% BSA, pH 7.5. Integrins (0.5–4.0 μg/ml) were allowed to bind for 1 h at 37°C. Next, the plates were washed three times with binding buffer and incubated with antiintegrin specific Mabs. The plates were washed three times with PBS and incubated with goat anti–mouse peroxidase–conjugated IgG for 1 h at 37°C. The plates were washed three times with PBS and ELISA substrate (OPD) was added and the OD was measured with an ELISA plate reader at a wavelength of 490 nm. All measurements were corrected for nonspecific binding to BSA and for reactivity with secondary antibody.

Statistical analysis

Statistical analysis was performed using Student's t test. P values <0.05 were considered significant.

References

Blood, C.H., and B.R. Zetter. 1990. Functional interactions with the vasculature: angiogenesis and tumor metastasis. *Biochim. Biophys. Acta.* 1032:89–118.

Bowersox, J.C., and N. Sorgenete. 1982. Chemotaxis of aortic endothelial cells in response to fibronectin. *Cancer Res.* 42:2547–2551.

Brooks, P.C., A.M.P. Montgomery, M. Rosenfeld, R.A. Reisfeld, T. Hu, G. Klier, and D.A. Cheresh. 1994. Integrin αvβ3 antagonists promote tumor regression by inducing apoptosis of angiogenic blood vessels. *Cell.* 79:1157–1164.

Brooks, P.C., S. Stromblad, L.C. Sanders, T.L. von Schalscha, R.T. Aimes, W.G. Stetler-Stevenson, J.P. Quigley, and D.A. Cheresh. 1996. Localization of matrix metalloproteinase MMP-2 to the surface of invasive cells by interaction with integrin. *Cell.* 85:683–693.

Brooks, P.C., A.M.P. Montgomery, and D.A. Cheresh. 1998. Use of the 10 day old chick embryo model for studying angiogenesis. A.R. Howlett, editor. Humana Press Inc., Totowa, NJ. 257–269.

Davis, G.E. 1992. Affinity of integrins for damaged extracellular matrix: αvβ3 binds to denatured collagen type I through RGD sites. *Biochem. Biophys. Res. Commun.* 182:1025–1031.

Davis, G.E., K.J. Bayless, M.J. Davis, and G.A. Meiniger. 2000. Regulation of tissue injury responses by the exposure of matricryptic sites within extracellular matrix molecules. *Am. J. Pathol.* 156:1489–1498.

Dipietro, L.A., M. Burdick, Q.E. Low, S.L. Kunkel, and R.M. Strieter. 1998. MIP-1α as a critical macrophage chemoattractant in murine wound repair. *J. Clin. Invest.* 101:1693–1698.

Dogic, D., B. Eckes, and M. Aumailley. 1999. Extracellular matrix, integrins and focal adhesions. *Curr. Top. Pathol.* 93:75–83.

Emsley, J., G. Knight, R.W. Farndale, M.J. Barnes, and R.C. Liddington. 2000. Structural basis of collagen recognition by integrin α2β1. *Cell.* 100:47–56.

Friedlander, M., C.L. Theesefeld, M. Sugita, M. Fruttiger, M.A. Thomas, S. Change, and D.A. Cheresh. 1996. Involvement of integrins αvβ3 and αvβ5 in ocular neovascular diseases. *Proc. Natl. Acad. Sci. USA.* 93:9764–9769.

Giannelli, G., J. Falk-Marzillier, O. Schiraldi, W.G. Stetler-Stevenson, and V. Quaranta. 1997. Induction of cell migration by matrix metalloproteinase-2 cleavage of laminin-5. *Science.* 277:225–228.

Hanahan, D., and J. Folkman. 1996. J. Patterns and emerging mechanisms of the angiogenic switch during tumorigenesis. *Cell.* 86:353–364.

Herbst, T.J., J.B. McCarthy, E.C. Tsilbary, and L.T. Furcht. 1998. Differential effects of laminin, intact type IV collagen, and specific domains of type IV collagen on endothelial cell adhesion and migration. *J. Cell Biol.* 106:1365–1373.

Hiraoka, N., E. Allen, I.J. Apel, M.R. Gyetko, and S.J. Weiss. 1998. Matrix metalloproteinases regulate neovascularization by acting as pericellular fibrinolysins. *Cell.* 95:365–377.

Hudson, B.G., S.T. Reeders, and K.J. Tryggvason. 1993. Type IV collagen: structure, gene organization, and role in human diseases. *J. Biol. Chem.* 268:26033–26036.

Itoh, T., M. Tanioka, H. Yoshida, T. Yoshioka, H. Nishimoto, and S. Itohara. 1998. Reduced angiogenesis and tumor progression in gelatinase A-deficient mice. *Cancer Res.* 58:1048–1051.

Jukkola, A., R. Taktela, E. Tholix, K. Vuorinen, G. Blanco, L. Risteli, and J. Risteli. 1997. Aggressive breast cancer leads to discrepant serum levels of the type I procollagen propeptides PINP and PICP. *Cancer Res.* 57:5517–5520.

Koch, A.E., M.M. Halloran, C.J. Haskell, S.R. Manisha, P.J. Polverini. 1995. Angiogenesis mediated by soluble forms of E-selectin and vascular cell adhesion molecule-1. *Nature.* 376:517–519.

Liotta, L.A., P.A. Steeg, and W.G. Stetler-Stevenson. 1991. Cancer metastasis and angiogenesis: an imbalance of positive and negative regulation. *Cell.* 64:327–336.

Messent, A.J., D.S. Tuckwell, V. Knauper, M.J. Humphries, G. Murphy, and J. Gavrilovic. 1998. Effects of collagenase-cleavage of type I collagen on α2β1 integrin mediated cell adhesion. *J. Cell Sci.* 111:1127–1135.

Montgomery, A.M.P., R.A. Reisfeld, and D.A. Cheresh. 1994. Integrin αvβ3 rescues melanoma cells from apoptosis in a three-dimensional dermal collagen. *Proc. Natl. Acad. Sci. USA.* 91:8856–8860.

O'Reilly, M.S., M.S. Holmgren, L. Shing, Y. Chen, R.A. Rosenthal, M. Moszes, W.W. Lane, Y. Cao, E.H. Sage, and J. Folkman. 1994. Angiostatin: a novel angiogenesis inhibitor that mediates the suppression of metastases by lewis lung carcinoma. *Cell.* 79:315–328.

Petitclerc, E., S. Stromblad, T.L. von Schalsacha, F. Mitjans, J. Piutats, A.M.P. Montgomery, D.A. Cheresh, and P.C. Brooks. 1999. Integrin αvβ3 promotes M21 melanoma growth in human skin by regulating tumor cell survival. *Cancer Res.* 59:2724–2730.

Rak, J., J. Filmus, G. Finkenzeller, S. Grugel, D. Marme, and R.S. Kerbel. 1995. Oncogenes as inducers of tumor angiogenesis. *Cancer Metastasis Rev.* 14: 263–277.

Risau, W., and V. Lemmon. 1988. Changes in vascular extracellular matrix during embryonic vasculogenesis and angiogenesis. *Dev. Biol.* 125:441–450.

Schnaper, W.H., D.S. Grant, W.G. Stetler-Stevenson, R. Fridaman, G. D'razi, A.N. Murphy, R.E. Bird, M. Hoythya, T.R. Fuerst, D.L. French, J.P. Quigley, and H.K. Kleinman. 1993. Type IV collagenases and TIMPs modulate endothelial cell morphogenesis in vitro. *J. Cell. Physiol.* 156:235–246.

Senger, D.R., and C.A. Perruzzi. 1996. Cell migration promoted by a potent RGDS-containing thrombin-cleavage fragment of osteopontin. *Biochim. Biophys. Acta*. 1314:13–24.

Smith, J.W., and D.A. Cheresh. 1988. The Arg-Gly-Asp binding domain of the vitronectin receptor. *J. Biol. Chem.* 263:18726–18731.

Stetler-Stevenson, W.G. 1999. Matrix metalloproteinases in angiogenesis: a moving target for therapeutic intervention. *J. Clin. Invest.* 103:1237–1241.

Suri, C., P.F. Jones, S. Patan, S. Bartunkova, P.C. Maisonpierre, S. Davis, T.N. Sato, and G.D. Yancopoulos. 1996. Requisite role of Angiopoietin-1, a ligand for the TIE2 receptor, during embryonic angiogenesis. *Cell.* 87: 1171–1180.

Timpl, R. 1996. Macromolecular organization of basement membranes. *Curr. Opin. Cell Biol.* 8:618–624.

Timpl, R., and J.C. Brown. 1995. Supramolecular assembly of basement membranes. *Bioessays*. 18:123–132.

Tsai, L.-H. 1998. Stuck on the ECM. *Trends Cell Biol*. 8:192–295.

Vu, T., M.J. Shipley, G. Bergers, J.E. Berger, J.A. Helms, D. Hanahan, S.D. Shapiro, R.M. Senior, and Z. Werb. 1998. MMP-9/gelatinase B is a key regulator of growth plate angiogenesis and apoptosis of hypertrophic chondrocytes. *Cell.* 93:411–422.

Weidner, N., J.P. Semple, W.R. Welch, and J. Folkman. 1991. Tumor angiogenesis and metastasis, correlation in invasive breast carcinoma. *N. Engl. J. Med.* 324:1–8.

Weidner, N., J. Folkman, F. Pozza, P. Bevilacqua, E.N. Allred, D.H. Moore, S. Meli, and G. Gasparini. 1992. Tumor angiogenesis: a new significant and independent prognostic indicator in early-stage breast carcinoma. *J. Natl. Cancer Inst.* 84:1875–1887.

Werb, Z., T. Vu, J.L. Rinkenberger, and L.M. Coussens. 1999. Matrix-degrading proteases and angiogenesis during development and tumor formation. *APMIS*. 107:11–18.

Xu, J., D. Rodriguez, J.J. Kim, and P.C. Brooks. 2000. Generation of monoclonal antibodies to cryptic collagen sites by using subtractive immunization. *Hybridoma*. 19:375–385.

Xu et al. Vol. 154, No. 5, September 3, 2001. Pages 1069–1079.

Due to an editorial oversight, an author name was misprinted as "S. Moon Yuen." The correct name is "Yeon Sung Moon." The accurate author line appears below.

Jingsong Xu,[1] Dorothy Rodriguez,[1] Eric Petitclerc,[1] Jenny J. Kim,[1] Masanori Hangai,[2] Yeon Sung Moon,[2] George E. Davis,[3] and Peter C. Brooks[1]